Dynamical Screening and Excitonic Instability in Bilayer Graphene

Dynamical Screening and Excitonic Instability in Bilayer Graphene

Rahul Nandkishore and Leonid Levitov

Department of Physics, Massachusetts Institute of Technology, 77 Massachusetts Avenue, Cambridge, Massachusetts 02139, USA

(Received 30 July 2009; revised manuscript received 11 December 2009; published 15 April 2010)

Electron interactions in undoped bilayer graphene lead to an instability of the gapless state, ''which-layer'' symmetry breaking, and energy gap opening at the Dirac point. In contrast with single-layer graphene, the bilayer system exhibits instability even for an arbitrarily weak interaction. A controlled theory of this instability for realistic dynamically screened Coulomb interactions is developed, with full account of the dynamically generated ultraviolet cutoff. This leads to an energy gap that scales as a power law of the interaction strength, making the excitonic instability readily observable.

DOI: 10.1103/PhysRevLett.104.156803 PACS numbers: 73.22.Pr, 73.21.−b

Graphene, due to its unique electronic structure of a two-dimensional semimetal, provides an entirely new setting for investigating many-body phenomena [1]. Since the conduction and valence band joined together in a semimetal mimic massless Dirac particles, electronic phenomena in graphene often have direct analogs in high energy physics [2]. In particular, several authors discussed the analogy between excitonic instability in a single-layer graphene and chiral symmetry breaking in $2 + 1$ quantum electrodynamics. While this instability is absent when interactions are weak [3], and the situation for realistic interaction strength is still debated, the instability can be ''catalyzed'' by a magnetic field [4,5]. These predictions are in qualitative agreement with experiment [6].

The effect of interactions is drastically different for semimetals with linear (type I) and quadratic (type II) electron dispersion. This was recognized in an early work [7], where the difference in behavior was traced to the density of states at low energies, which is much lower in type I systems than in type II systems. Electronic properties of quadratically dispersing systems are governed by infrared divergences in Feynman diagrams, resulting in unconventional low-energy states, whereas in linearly dispersing systems the free-particle description is robust. Indeed, excitonic instability in bilayer graphene (BLG), which has gapless quadratically dispersing electronic states, was shown to occur for arbitrarily weak short range repulsion [8].

In this Letter, we analyze excitonic instability in a BLG system with $1/r$ interaction, focusing on a ferroelectric (FE) state that spontaneously breaks which-layer symmetry and polarizes the layers in charge. After accounting for dynamically generated ultraviolet cutoff, treated in the RPA screening framework, we find a gap which in the weak coupling limit scales as a square of the interaction strength, $\Delta \propto (e^2/\kappa)^2$, with e the electron charge and κ the dielectric constant. This is in contrast to the exponential BCS-like behavior of the gap expected in single layers coupled via a dielectric spacer [9–11].

Interestingly, we find the behavior to be highly sensitive to the specifics of screening model: log divergent diagrams can become $\log^2$ divergent upon going from static to dynamic screening [see Fig. 1(b)]. Thus for a reliable estimate of the gap it is necessary to properly treat dynamic screening. We evaluate the dynamical polarization function for BLG and use it to estimate the gap value. For realistic parameters the predicted gap lies within the experimentally accessible range. Generalizing our approach for the antiferromagnetic (AF) states considered in [8], we find that the AF and FE states are nearly degenerate in energy.

The formation of a gapped state will manifest itself in strongly temperature dependent conductivity at $T \lesssim \Delta$. In the presence of long-range disorder, the gapped state will occur at the p-n boundaries separating electron and hole ''puddles,'' making these boundaries a bottleneck for transport. Hopping-like temperature dependence is indeed noted in all conductivity measurements near the neutrality point in BLG but not in single-layer graphene [1].

Since the ferroelectric transition breaks a Z_2 symmetry, excitonic ordering will produce domains of opposite polarization [see Fig. 1(a)]. In the absence of disorder, the characteristic size of the domains L is determined by long-range attraction between polarization in neighboring domains, in analogy with ''electronic microemulsion phases'' discussed in Ref. [12], giving an estimate $8\rho^2 \ln(L/a_0) \approx \Delta/a_0$, where ρ is polarization density and a_0 is the corre-

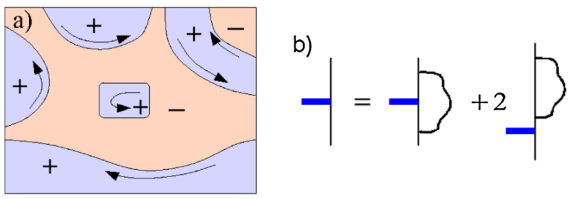

FIG. 1 (color online). (a) Domains of opposite polarization in the ferroelectric state. Valley polarized chiral edge states propagate in opposite directions along domain boundaries. (b) Diagrammatic representation of gap equation. First term is vertex correction, second term is self-energy correction. Both diagrams exhibit $\log^2$ divergence which cancel to leading order. Solid, wavy, and thick lines represent fermion propagators, the RPA interaction (4), and $\Delta\tau_3$ vertex, respectively.

lation length, Eq. (3). As discussed in Ref. [13], the boundaries between regions with opposite polarization host valley polarized edge states. Since a two-dimensional system with two domain types should exhibit percolation of edge states, the FE state should be able to carry valley currents. This could be useful for valleytronics applications.

The low-energy Hamiltonian for BLG can be described in a "two band" approximation, neglecting the higher bands that are separated from the Dirac point by an energy gap $W \sim 0.4$ eV [14]. The electron states are described by wave function taking values on the A and B sublattice of the upper and lower layer, respectively. The noninteracting spectrum consists of quadratically dispersing quasiparticle bands $E_{\pm} = \pm p^2/2m$ with band mass $m \approx 0.054 m_e$. It is convenient to introduce the Pauli matrices τ_i that act on the sublattice space, and to define $\tau_{\pm} = (\tau_1 \pm i\tau_2)/2$ and $p_{\pm} = p_x \pm i\zeta p_y$ [14], where $\zeta = 1$ for the K valley and $\zeta = -1$ for the K' valley. The Hamiltonian may then be written as

$$H_0 = \sum_{\mathbf{p},\alpha} \psi^{\dagger}_{\mathbf{p},\alpha} \left(\frac{p_+^2}{2m}\tau_+ + \frac{p_-^2}{2m}\tau_- \right) \psi_{\mathbf{p},\alpha},$$
$$H = H_0 + \frac{e^2}{2\kappa} \sum_{x,x'} \frac{n(\mathbf{x}) n(\mathbf{x}')}{|\mathbf{x} - \mathbf{x}'|}, \quad n(\mathbf{x}) = \sum_{\alpha} \psi^{\dagger}_{\alpha}(\mathbf{x}) \psi_{\alpha}(\mathbf{x}). \tag{1}$$

The sum over α indicates summation over $N = 4$ spin and valley species, while the dielectric constant κ incorporates the effect of polarization of the substrate and of the higher bands of BLG. The interaction is invariant under $SU(N)$ rotations in spin-valley space. We also approximate by treating the interlayer and intralayer interaction as equal, and defer discussing the effect of finite layer separation until after we present our main result.

We investigate stability of the gapless state by introducing a test gap-opening perturbation $\Delta\tau_3$ into the noninteracting Hamiltonian, where Δ must be real, but may take either sign. This test perturbation explicitly breaks the Z_2 layer symmetry of the Hamiltonian, and corresponds to a ferroelectric instability that polarizes the layers by charge. We develop our analysis perturbatively in the interaction, and calculate the interaction renormalization of the $\Delta\tau_3$ vertex. At leading order in weak bare interactions, the vertex correction in Fig. 1(b) takes the form $\delta\Gamma = \tau_3 \delta\Delta$, where

$$\delta\Delta = -\int \frac{\Delta}{(iE + H_0)(iE - H_0)} U. \tag{2}$$

Here H_0 is the Hamiltonian of the noninteracting system evaluated at $\Delta = 0$. The vertex correction is positive and preserves the form of the σ_3 vertex. Moreover, simple power counting shows that the vertex correction is divergent in the infrared for any form of interaction U, screened or unscreened. The infrared divergence indicates instability even for arbitrarily weak interactions (unlike monolayer graphene). The infrared divergence is power law when U is the unscreened Coulomb interaction; therefore, it is important to include screening even at weak coupling, to moderate the infrared divergence.

We now introduce the interaction energy scale E_0 and the corresponding length scale a_0, defined as

$$E_0 = \frac{me^4}{\kappa^2\hbar^2} \approx \frac{1.47}{\kappa^2}\,\text{eV}, \quad a_0 = \frac{\kappa\hbar^2}{me^2} \approx \kappa \times 1.1\,\text{nm}. \tag{3}$$

For simplicity, we take the weak coupling limit $E_0 \lesssim W$, and neglect interaction-induced mixing of the low-energy states with the higher bands [for discussion of mixing see Ref. [15]]. Moreover, when U is the unscreened or dynamically screened Coulomb interaction, the integral in Eq. (2) is convergent in the ultraviolet limit, without the need for any high energy cutoff. Thus E_0 emerges as the only energy scale in the problem. This then implies that the energy scale for the gap must scale as a power law in electric charge $\Delta \sim E_0 \sim e^4$.

As we shall see, it is necessary to properly treat dynamic screening to obtain a reliable estimate for the gap. We therefore take U in Eq. (2) to be the dynamically screened Coulomb interaction, defined as

$$\tilde{U}_{\omega,\mathbf{q}} = \frac{2\pi e^2}{\kappa q - 2\pi e^2 N \Pi_{\omega,\mathbf{q}}}. \tag{4}$$

Here we have introduced the single species polarization function $\Pi_{\omega,\mathbf{q}} = -\int G(\mathbf{p}_+, \varepsilon_+) G(\mathbf{p}_-, \varepsilon_-) \frac{d\varepsilon d^2p}{(2\pi)^3}$, where we use the notation $\mathbf{p}_{\pm} = \mathbf{p} \pm \mathbf{q}/2$ and $\varepsilon_{\pm} = \varepsilon \pm \omega/2$, and define the imaginary frequency Green function in terms of the noninteracting Hamiltonian H_0 as $G^{-1}(E, \mathbf{p}, \Delta) = iE - H_0(\mathbf{p}, \Delta)$. Hence, we obtain

$$\Pi_{\omega,\mathbf{q},\Delta} = -2\int \frac{dE d^2p}{(2\pi)^3} \frac{E_+E_- - p_+^2 p_-^2 \cos(2\theta_{pq}) - \Delta^2}{(E_+^2 + p_+^4 + \Delta^2)(E_-^2 + p_-^4 + \Delta^2)}. \tag{5}$$

Here, θ_{pq} is the angle between the vectors $\mathbf{p}_+$ and $\mathbf{p}_-$. To determine the dynamically screened interaction, it is sufficient to determine the polarization function in the ungapped state. We therefore suppress Δ in Eq. (5), integrate over frequencies by residues, and scale out q. The integral then depends on a single dimensionless parameter $\tilde{\omega} = 2m\omega/q^2$, and may be evaluated analytically by integrating over momenta in polar coordinates [16]. This gives an exact expression for the polarization function $\Pi_{\omega,\mathbf{q},0} = -\frac{m}{2\pi} f(\tilde{\omega})$, where

$$f(\tilde{\omega}) = \frac{2\tan^{-1}\tilde{\omega} - \tan^{-1} 2\tilde{\omega}}{\tilde{\omega}} + \ln\frac{\tilde{\omega}^2 + 1}{\tilde{\omega}^2 + \frac{1}{4}} \approx \frac{\ln 4}{\sqrt{1 + u\tilde{\omega}^2}}, \tag{6}$$

where $u = (2\ln 4/\pi)^2$. The right-hand side provides an approximate formula that reproduces $f(\tilde{\omega})$ exactly for $\tilde{\omega} \to 0$ and $\tilde{\omega} \to \infty$, interpolating accurately between the two limits. Result (6) agrees with the polarization function found in [17] continued to Matsubara frequencies.

The vertex correction, Eq. (2), calculated with the dynamically screened interaction, Eq. (4), is $\log^2$ divergent in

the infrared [16]. The enhanced divergence arises from the phase space region $\omega/q^2 \gg 1$, where the Coulomb interaction is not efficiently screened. However, it is also necessary to take account of the self-energy correction, so that the full gap equation is represented by Fig. 1(b). In particular, the self-energy undergoes a $\log^2$ renormalization [18], and this can be shown to cancel the vertex correction at $\log^2$ order, leaving a residual logarithmic divergence.

Since demonstrating the cancellation of the self-energy and vertex correction at leading $\log^2$ order and extracting the subleading logarithmic divergence is fairly tedious, we employ an alternative scheme for solving the gap equation Fig. 1(b). We note that calculating the free energy of BLG as a function of Δ, at leading nonvanishing order in Δ, simply produces the diagrams in Figs. 2(a)–2(c). Upon minimizing with respect to Δ, this yields the gap equation, pictured in Fig. 1(b), with correct combinatorial coefficients. Minimizing the free energy of BLG with respect to Δ is therefore formally equivalent to solving the gap equation, and is technically simpler. It may be verified that while Figs. 2(b) and 2(c) are individually $\log^3$ divergent in the infrared, their sum is only $\log^2$ divergent. This is the same leading order cancellation of divergences that is manifested by the gap equation, Fig. 1(b).

We approximate by assuming that the gap function Δ is static and momentum independent up to energies of order E_0, on the grounds that the screened interaction in the particle-hole channel depends only weakly on the transferred momentum. We evaluate the kinetic energy change δT represented by Fig. 2(a) by including Δ in the fermion Green function. We find, with logarithmic accuracy, $\delta T = \frac{m}{2\pi}\Delta^2 \ln(\Lambda/\Delta)$, with the cutoff $\Lambda \sim E_0$.

To calculate the exchange energy gain, we note that the difference in interaction energy between the gapped and ungapped states, $\delta E = E(\Delta) - E(0)$ is given, within the RPA approach, by

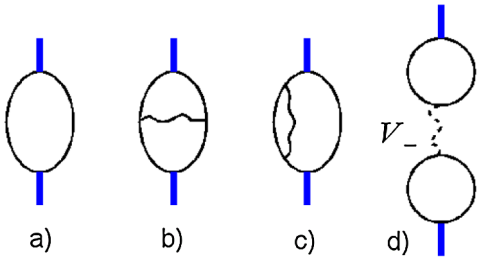

FIG. 2 (color online). Free energy change from gap formation at leading order in Δ and in the interaction (notation the same as in Fig. 1). The diagrams may be interpreted as (a) kinetic energy cost from spontaneous gap opening; (b),(c) interaction energy gain from gap opening; (d) Hartree energy cost of layer polarization, which vanishes within the approximations of Eq. (1). Here V_- is the difference between interlayer and intralayer interactions. While all these diagrams are nominally $O(\Delta^2)$, Δ also appears as a logarithmic infrared cutoff in each diagram, Eq. (9).

$$\delta E = \int \frac{d\omega d^2p}{(2\pi)^3} \ln[1 - N\tilde{U}_{\omega,q}(\Pi_{\omega,q,\Delta} - \Pi_{\omega,q,0})]. \quad (7)$$

Here, $\tilde{U}_{\omega,q}$ is the interaction (4) and $\Pi_{\omega,q,\Delta}$ is the single species polarization function in the gapped state. The problem thus reduces to that of evaluating the polarization function at finite Δ.

We calculate the quantity $\Pi_\Delta - \Pi_0$ by integrating Eq. (5) over frequencies by residues, Taylor expanding to leading order in small Δ^2, and analytically performing the integration over momenta, assuming as before that Δ is independent of momentum. After some algebra [16], we obtain

$$\Pi_\Delta - \Pi_0 = \frac{m\Delta^2}{2\pi r^2}\left(-7\frac{q^4}{r^2} + 4\frac{q^8}{r^4}\right)\ln\frac{r}{\Delta}. \quad (8)$$

We are using the notation $r^2 = \omega^2 + q^4$.

We now evaluate the exchange energy gain from gap formation by substituting Eq. (8) into Eq. (7), and performing the integrals using polar coordinates [16]. Combining this with the kinetic energy cost δT, we find the free energy associated with gap opening

$$F(\Delta) = \frac{m}{2\pi}\Delta^2 \ln(\Lambda/\Delta) - \frac{13m\Delta^2}{6\pi^3}\ln^2(N^2E_0/\Delta). \quad (9)$$

We note the expected emergence of a natural ultraviolet cutoff. Identifying Λ with N^2E_0, and minimizing Eq. (9) with respect to Δ, we obtain, with logarithmic accuracy,

$$\Delta = N^2E_0 \exp(-3\pi^2 N/13). \quad (10)$$

We emphasize that E_0 appears only outside the exponential, making Δ a power law function of interaction strength at weak coupling. However, Δ is exponentially small in N, where N is the number of fermion species participating in screening. If we had worked instead with static screening, we would have obtained $\Delta \sim N^2E_0 \exp(-2N \ln 4)$, and would have underestimated the size of the gap by an order of magnitude.

For $N = 4$ Eq. (10) gives $\Delta \approx 10^{-3}E_0 \approx 1.5\kappa^{-2}$ meV, up to a numerical prefactor of order unity. Meanwhile, numerically evaluating the integrals in Eq. (7) and the kinetic energy contribution δT [Fig. 2(a)], and minimizing the free energy gives $\Delta \approx 4\kappa^{-2}$ meV. This number lies within experimentally accessible range, although it can be reduced by screening in the substrate, by doping, or by disorder induced density inhomogeneity.

Thus far, we have neglected the effect of trigonal warping which leads to deviation of particle dispersion from a simple quadratic dependence, causing an overlap of the conduction and valence bands. Trigonal warping can provide an alternative low-energy cutoff, preventing formation of a gapped state if its size exceeds the estimated gap. Since the upper estimate for trigonal warping, 1.5 meV [19], is less than the numerical estimate $\Delta \approx 4\kappa^{-2}$ meV, the effect of trigonal warping should be inessential, at least for suspended bilayers ($\kappa \approx 1$).

Our analysis can be easily generalized to any state that adds a term $\Delta\tau_3\Omega$ to the Hamiltonian (1), where Ω is a 4×4 Hermitian matrix in spin and valley space satisfying $\Omega^2 = 1$. The FE state considered above corresponds to $\Omega = 1$, whereas the AF states discussed in Ref. [8] are characterized by $\Omega = \sigma_3 \otimes 1$ or $\Omega = 1 \otimes \eta_3$, where σ_3 and η_3 are Pauli matrices in spin and valley space, respectively. All these inequivalent choices for Ω yield the same mean field free energy $F(\Delta)$, Eq. (9), and the same gap value as was obtained for the FE state. This mean field degeneracy occurs because the Hamiltonian is invariant under $SU(4)$ spin-valley rotations, within validity of Eq. (1), while the states corresponding to different choices of Ω differ only in their spin and valley structure [22].

We now examine the effect of finite layer separation $d \approx 3$ Å, which differentiates the interlayer and intralayer interactions, giving an anisotropy $V_- = \frac{1}{2}(V_{AA} - V_{AB}) = \frac{1}{2}\frac{2\pi e^2}{q}(1 - e^{-qd}) = \pi e^2 d$. This anisotropy is small, because $d \ll a_0$. The leading order effect of finite layer separation is to introduce a Hartree energy for the states that polarize the layers in charge [see Fig. 2(d)],

$$E_{\text{Hartree}} = \frac{Nm^2}{4\pi^2} V_- \Delta^2 \ln^2(\Lambda/\Delta). \tag{11}$$

It was argued in Ref. [19] that this contribution prevents formation of the ferroelectric state. However, Ref. [19] neglected the exchange energy. We note that the Hartree energy is of the same functional form as the exchange energy, Eq. (9), but is parametrically smaller by $d/a_0 \ll 1$, and so cannot prevent the instability.

Upon going beyond the weak coupling approximation, d/a_0 ceases to be a good control parameter, but our conclusions remain unchanged. This is because the V_- interaction is screened as $\tilde{V}_- = V_-/(1 - V_-\Pi_-)$, where $\Pi_- = \int \mathrm{Tr} G(\varepsilon_+, p_+)\tau_3 G(\varepsilon_-, p_-)\tau_3 \frac{d\varepsilon d^2p}{(2\pi)^3} \sim \frac{m}{2\pi}\ln(\Lambda/\Delta)$. Such logarithmic screening ensures that the Hartree energy remains smaller than the exchange energy, Eq. (9), and so cannot prevent gap formation. However, when d/a_0 is not small, the Hartree energy may tip the balance from the FE state to one of the AF states, which do not polarize the layers by charge.

A ferromagnetic instability was predicted for unscreened interactions in [17]. However, the free energy gain from ferromagnetism was only cubic in the ferromagnetic order parameter. In contrast, the excitonic states all have a free energy gain of $O(\Delta^2)$, and should thus dominate for weak coupling.

To conclude, we have demonstrated that electron interactions drive BLG to a gapped state. For dynamically screened Coulomb interactions, taking proper account of dynamically generated ultraviolet cutoff and $\log^2$ divergences arising in this case, we obtain a gap value in experimentally accessible range ($\Delta \approx 4\kappa^{-2}$ meV). Manifestations of the energy gap-opening in BLG at charge neutrality include temperature dependent transport at low temperatures, and also valley polarized chiral edge states propagating along domain boundaries.

We acknowledge useful discussions with D. Abanin, P. A. Lee, Nan Gu, D. Mross, and A. Potter. This work was supported by Office of Naval Research Grant No. N00014-09-1-0724.

Note added.—Recently we became aware of works [20,21]. Instabilities in BLG are analyzed in these papers within a renormalization group framework, with interactions modeled as being short range. It is found that different choices of short range interaction can result in different states, gapped [20] or gapless [21].

[1] A. K. Geim and K. S. Novoselov, Nature Mater. **6**, 183 (2007).
[2] J. Gonzalez, F. Guinea, and M. A. H. Vozmediano, Nucl. Phys. **B424**, 595 (1994); Phys. Rev. B **59**, R2474 (1999).
[3] D. V. Khveshchenko, Phys. Rev. Lett. **87**, 246802 (2001).
[4] V. P. Gusynin, V. A. Miransky, and I. A. Shovkovy, Phys. Rev. Lett. **73**, 3499 (1994).
[5] I. F. Herbut, Phys. Rev. Lett. **97**, 146401 (2006).
[6] J. G. Checkelsky, L. Li, and N. P. Ong, Phys. Rev. Lett. **100**, 206801 (2008).
[7] A. A. Abrikosov and S. D. Beneslavskii, Zh. Eksp. Teor. Fiz. **59**, 1280 (1970) [Sov. Phys. JETP **32**, 4 (1971)]; J. Low Temp. Phys. **5**, 141 (1971).
[8] H. Min, G. Borghi, M. Polini, and A. MacDonald, Phys. Rev. B **77**, 041407(R) (2008).
[9] H. Min, R. Bistritzer, J. J. Su, and A. H. MacDonald, Phys. Rev. B **78**, 121401(R) (2008).
[10] C. H. Zhang and Y. N. Joglekar, Phys. Rev. B **77**, 233405 (2008).
[11] M. Y. Kharitonov and K. B. Efetov, Phys. Rev. B **78**, 241401(R) (2008).
[12] R. Jamei, S. Kivelson, and B. Spivak, Phys. Rev. Lett. **94**, 056805 (2005).
[13] I. Martin, Y. M. Blanter, and A. F. Morpurgo, Phys. Rev. Lett. **100**, 036804 (2008).
[14] E. McCann and V. Fal'ko, Phys. Rev. Lett. **96**, 086805 (2006); E. McCann, Phys. Rev. B **74**, 161403(R) (2006).
[15] D. S. L. Abergel and T. Chakraborty, Phys. Rev. Lett. **102**, 056807 (2009).
[16] See supplementary material at http://link.aps.org/supplemental/10.1103/PhysRevLett.104.156803 for algebraic details regarding the calculations presented.
[17] J. Nilsson, A. H. Castro Neto, N. M. R. Peres, and F. Guinea, Phys. Rev. B **73**, 214418 (2006).
[18] Y. Barlas and K. Yang, Phys. Rev. B **80**, 161408(R) (2009).
[19] E. McCann, D. S. L. Abergel, and V. Falko, Solid State Commun. **143**, 110 (2007).
[20] F. Zhang, H. Min, M. Polini, and A. H. MacDonald, Phys. Rev. B **81**, 041402(R) (2010).
[21] O. Vafek and K. Yang, Phys. Rev. B **81**, 041401(R) (2010).
[22] R. Nandkishore and L. Levitov, arXiv:1002.1966.